Inorg. Chem. **2007**, *46*, 7285–7293

Synthesis and Relative Stability of a Series of Compounds of Type [Fe(II)(bztpen)X]$^+$, Where bztpen = Pentadentate Ligand, N_5, and X^- = Monodentate Anion

Norma Ortega-Villar,[‡] Víctor M. Ugalde-Saldívar,[‡] M. Carmen Muñoz,[§] Luis A. Ortiz-Frade,[‡] José G. Alvarado-Rodríguez,[||] José A. Real,[†] and Rafael Moreno-Esparza*[,‡]

Universitat de València, Instituto de Ciencia Molecular, Edificio de Institutos de Paterna, Apartado de correos 22085, 46071 València, Spain, Facultad de Química (UNAM), Edificio B. Av. Universidad 3000, Coyoacán, México D. F. 04510, México, Departament de Física Aplicada. Universitat Politécnica de València, Camino de Vera s/n, E-46022 València, Spain, and Centro de Investigaciones Químicas, Universidad Autónoma del Estado de Hidalgo, Ciudad Universitaria km. 4.5, Carretera Pachuca-Tulancingo 42074, Pachuca, Hidalgo, México

Received October 30, 2006

The structural and solution characterization of novel Fe(II) compounds of the general formula [Fe(bztpen)X]PF_6 and [Fe(bztpen)CH_3CN]$(PF_6)_2$ is presented, where bztpen is the pentadentate ligand *N*-benzyl-*N*,*N*′,*N*′-tris(2-methylpyridyl)ethylenediamine and X^- is a monodentate ligand. All complexes were characterized in solution and in the solid state, employing the usual techniques and single-crystal X-ray diffraction. The results obtained are discussed in terms of the existing information for some previously reported analogous compounds to arrive at a rationalization regarding the influence of a variation in the coordination environment of all compounds and to evaluate their relative stability. The observed magnetic response in the solid state is paramagnetic in the entire temperature range for the Cl^-, Br^-, I^-, OCN^-, and SCN^- derivatives, while the $N(CN)_2^-$, CH_3CN, and CN^- derivatives are diamagnetic. The diamagnetic character of these last two compounds is confirmed in acetonitrile solution, while a spin transition step is observed for the $N(CN)_2^-$ derivative. Diffraction data for all compounds as hexafluorophosphates shows that the I^-, Br^-, and OCN^- derivatives crystallize in the orthorhombic space group *Pbca*, while the CN^-, SCN^-, and CH_3CN compounds crystallize in the triclinic space group $P\bar{1}$. Average bond lengths and the trigonal distortion parameter can be correlated to the observed magnetic susceptibility depending on the coordinated monodentate ligand. Solution measurements of electronic properties for the compounds follow the trend established by the spectrochemical series. The relative stability of the Fe(II) complexes can be established in terms of the percentage of dissociation from the voltammetry and conductivity results, which are consistent with those obtained spectrophotometrically, mainly, the larger stability for the CN^- derivative and the lower for the I^- derivative. The redox potential and percentage of dissociation values allow for the estimation of the relative stability constants for the Fe(II) and Fe(III) complexes.

Introduction

The study of mononuclear complexes of Fe(II) coordinated to polydentate ligands through nitrogen atoms (N_6 or N_5X) has, during the last fifteen years, yielded a fruitful research field with excellent results, especially in the magnetochemical area. To this day, there is a significant database of experimental and theoretical results, continuously mentioned and frequently employed, which has proven to be extremely useful to understand and correlate the magnetic behavior of these complexes with their structural parameters. Although several reviews on this subject have been published lately, the ongoing study of these systems does not fail to provide novel and interesting information.[1,2] In addition, solution studies of the magnetic behavior for these compounds are extremely scarce.

* To whom correspondence should be addressed. E-mail: moresp@servidor.unam.mx.
[†] Universitat de València.
[‡] Facultad de Química (UNAM).
[§] Universitat Politécnica de València.
[||] Universidad Autónoma del Estado de Hidalgo.

10.1021/ic0620743 CCC: $37.00
Published on Web 08/04/2007

Since the 1990s, hydroxyperoxidase-like behavior for the $[Fe(II)(R\text{-tpen})Cl]^+$-type compounds has been reported.[3] The proposed mechanism for this behavior includes substitution of the chloride ligand by the hydroxyperoxo radical (·OOH), with the consequent oxidation of Fe(II) to Fe(III).[3−8] These compounds also show superoxydismutase (SOD) activity.[9]

From the proposed mechanism, it seems reasonable to assume that a variation of the monodentate ligand should modulate both stability and redox properties in these compounds. Because only the chloride and bromide (**1** and **2**) derivatives have been studied previously,[6] the investigation of the aforementioned properties when different monodentate substituents X^- are employed is an interesting field that may extend the existing available information.

With that perspective in mind, we carried out the synthesis and characterization in the solid state and in solution of a new series of $[Fe(II)(bztpen)X]^{n+}$ compounds, where X = I^- (**3**), OCN^- (**4**), SCN^- (**5**), CH_3CN (**7**), and CN^- (**8**). The main aim is to evaluate the variation in properties such as magnetic behavior both in solid state and solution, $Fe-N_5$ and $Fe-L_6$ average bond distances, electronic absorption spectra, and redox potentials. The analysis of such parameters should render more arguments to establish a relationship between the studied properties. Consequently, these results may in future be employed in the enzymatic catalysis area of study.

The results obtained in this work will be compared to those previously reported for the compounds with X^- = Cl^-, Br^-,[6] and $N(CN)_2^-$ (dicyanamide) (**6**)[10] to analyze the coordination environment of each compound and to estimate its field strength. The analysis of the redox potential values should yield information indicative of the relative stability between the Fe(II) and Fe(III) complexes. Finally, the percentage of dissociation data for the monodentate ligand X^- exchanging with the solvent molecule for these complexes will be presented.

Experimental Section

Synthesis. All manipulations were performed under an argon atmosphere, using standard Schlenk techniques. Commercially available reagents and solvents (analytical grade) were used without prior purification. Acetonitrile and acetone solvents were HPLC grade. The ligand bztpen was prepared according to the literature procedure.[8] Synthesis of the compound with $N(CN)_2^-$ (**6**) was reported previously.[10] The syntheses of $[Fe(bztpen)X]PF_6$ compounds where X^- = Br^-, I^-, SCN^-, OCN^-, and CH_3CN was carried out according to the following reaction scheme

$$[Fe(H_2O)_6](BF_4)_2 + bztpen = [Fe(bztpen)H_2O](BF_4)_2 \cdot nH_2O +$$
$$X^-_{(excess)} + NH_4PF_{6(excess)} = [Fe(bztpen)X]PF_6 + 2NH_4BF_4$$

For the CH_3CN compound, liquid acetonitrile was added instead of X^-, and a slightly different procedure was employed, compared to that outlined below.

Preparation of $[Fe(bztpen)X]PF_6$ Compounds. The cationic complex $[Fe(bztpen)CH_3OH]^{2+}$ was prepared by the dropwise addition of a solution of $Fe(BF_4)_2 \cdot 6H_2O$ (0.08 g, 0.24 mmol in 5 mL methanol) to a solution of bztpen (0.10 g, 0.24 mmol in 10 mL methanol). The coordinated solvent molecule of the precursor $[Fe(bztpen)CH_3OH]^{2+}$ was then replaced with X^- by the in situ addition of a freshly prepared methanolic solution containing an excess of the corresponding potassium salt (∼0.1 M, 10−20 mL). For the CH_3CN derivative, 15−20 mL of spectroscopy grade acetonitrile was added. The resulting yellow (Cl^-, Br^-, I^-, OCN^-, and SCN^-) or brown ($N(CN)_2^-$ and CH_3CN) mixture was stirred for 20 min, after which a solution of NH_4PF_6 (0.12 g, 0.71 mmol) in methanol was added very slowly (20 mL). In some cases, the precipitate formed was removed by filtration. The resulting solution was slowly evaporated under argon during ∼36 h, in which time-lapse monocrystalline samples of each compound were obtained.

$[Fe(bztpen)Cl]PF_6$ (1). Yield: 0.087 g, 56%. Yellow crystals. FAB MS: *m/z* 498 $(M - PF_6^- - Cl^- + H_2O + e^-)^+$, 514 $(M - PF_6^-)^+$. Anal. Calcd for $C_{27}H_{29}N_5ClF_6PFe$: C, 49.13; N, 10.56; H, 4.40. Found: C, 49.60; N, 10.61; H, 4.46%. This compound has already been reported.[6]

$[Fe(bztpen)Br]PF_6$ (2). Yield: 0.063 g, 38%. Yellow crystals. FAB MS: *m/z* 498 $(M - PF_6^-Br^- + H_2O + e^-)^+$, 558 $(M - PF_6^-)^+$. Anal. Calcd for $C_{27}H_{29}N_5BrF_6PFe$: C, 46.02; N, 9.43; H, 4.12. Found: C, 46.52; N, 9.95; H, 4.07%.

$[Fe(bztpen)I]PF_6$ (3). Yield: 0.084 g, 47%. Yellow crystals. FAB MS: *m/z* 498 $(M - PF_6^- - I^- + H_2O + e^-)^+$, 606 $(M - PF_6^-)^+$. Anal. Calcd for $C_{27}H_{29}N_5IF_6PFe$: C, 43.14; N, 9.32; H, 3.86. Found: C, 43.12; N, 9.17; H, 3.65%.

$[Fe(bztpen)OCN]PF_6$, (4). Yield: 0.074 g, 47%. Yellow crystals. FAB MS: *m/z* 521 $(M - PF_6^-)^+$. Anal. Calcd for $C_{28}H_{29}N_6OF_6PFe$: C, 50.45; N, 12.61; H, 4.35. Found: C, 49.62; N, 12.62; H, 3.87%. IR (KBr): ν(OCN) 2212 cm^{-1}.

$[Fe(bztpen)SCN]PF_6$ (5). Yield: 0.104 g, 65%. Orange crystals. FAB MS: *m/z* 537 $(M - PF_6^-)^+$. Anal. Calcd for $C_{28}H_{29}N_6SF_6PFe$: C, 49.27; N, 12.32; H, 4.25. Found: C, 49.57; N, 12.06; H, 4.06%. IR (KBr): ν(SCN) 2036 cm^{-1}.

$[Fe(bztpen)CH_3CN](PF_6)_2$ (7). Yield: 0.047 g, 25%. Brown crystals. FAB MS: *m/z* 497 $(M - 2PF_6^- - CH_3CN + H_2O + e^-)^+$, 650 $(M - PF_6^- - CH_3)$. Anal. Calcd for $C_{29}H_{32}N_6F_{12}P_2Fe$: C, 42.98; N, 10.37; H, 3.98. Found: C, 42.94; N, 10.47; H, 4.31%. IR (KBr): ν(CN) 2268 cm^{-1}.

A slightly different technique was employed to obtain the cyanide (X^- = CN^-) compound, where a methanol-acetone solution of the $[Fe(\textit{bztpen})Cl]PF_6$ compound was used, with the following reaction scheme

(1) Batten, S. R.; Bjernemose, J.; Jensen, P.; Leita, B. A.; Murray, K. S.; Mourabaki, B.; Smith, J. P.; Toftlund, H. *Dalton Trans.* **2004**, *20*, 3370−3375.
(2) Toftlund, H.; McGarvey, J. J. *Top. Curr. Chem.* **2004**, *233*, 151−166.
(3) Bernal, I.; Jensen, I. M.; Jensen, K. B.; McKenzie, C. J.; Toftlund, H.; Tuchagues, J. P. *Dalton Trans.* **1995**, 3669−3675.
(4) Roelfes, G.; Vrajmasu, V.; Chen, K.; Ho, R. Y. N.; Rohde, J. U.; Zondervan, Chapter; la Crois, R. M.; Schudde, E. P.; Lutz, M.; Spek, A. L.; Hage, R.; Feringa, B. L.; Münck, E.; Que, L., Jr. *Inorg. Chem.* **2003**, *42*, 2639−2653.
(5) Costas, M.; Mehn, M. P.; Jensen, M. P.; Que, L., Jr. *Chem. Rev.* **2004**, *104*, 939−986.
(6) Hazell, A.; McKenzie, C. J.; Nielsen, L. P.; Schindler, S.; Weitzer, M. *J. Chem. Soc., Dalton Trans*. **2002**, 310−317.
(7) (a) Horner, O.; Jeandey, C.; Oddou, J.; Bonville, P.; McKenzie, C. J.; Lotour, J. M. *Eur. J. Inorg. Chem.* **2002**, *12*, 3278−3283. (b) Nielsen, A.; Larsen, F. B.; Bond, A. D.; McKenzie, C. J. *Angew. Chem., Int. Ed.* **2006**, *45*, 1602−1606.
(8) Duelund, L.; Hazell, R.; McKenzie, C. J.; Nielsen, L. P.; Toftlund, H. *J. Chem. Soc., Dalton Trans.* **2001**, 152−156.
(9) Tamura, M.; Urano, Y.; Kikuchi, K.; Higuchi, T.; Hirobe, M.; Nagano, T. *J. Organomet. Chem*. **2000**, *611*, 586−592.
(10) Ortega-Villar, N.; Thompson, A. L.; Muñoz, M. C.; Ugalde-Saldívar, V. M.; Goeta, A. E.; Moreno-Esparza, R.; Real, J. A. *Chem.—Eur. J.* **2005**, *11*, 5721−5734.

$$[Fe(bztpen)Cl]PF_6 + KCN_{(excess)} + NH_4PF_{6(excess)} = [Fe(bztpen)CN]PF_6 + KCl$$

[Fe(bztpen)CN]PF_6·H_2O·MeOH (8). Yield: 0.090 g, 54%. Red crystals. FAB MS: *m/z* 505 $(M - PF_6^- - H_2O - CH_3OH)^+$. Anal. Calcd for $C_{29}H_{35}N_6O_2F_6PFe$: C, 51.43; N, 12.00; H, 4.57. Found: C, 50.03; N, 12.06; H, 5.02%. IR (KBr): ν(CN) 2063 cm^{-1}.

Physical Measurements. All complexes were characterized using IR (Perkin-Elmer FT-IR spectrophotometer, 1605), FAB^+ (JEOL JMS-SX spectrometer, 102 A), elemental analysis (Fissons EA 1105 CHNS−O microanalyzer), UV−vis (Diode array HP 8493A spectrophotometer), solid-state magnetic susceptibility (SQUID Quantum Design MPMS2 susceptometer, 5.5 T, 1 T; in the temperature range of 1.8−300 K), solution magnetic susceptibility (Evans method[11,12] in a 400 MHz Varian Unity Inova NMR spectrometer), where both the internal reference and the sample (10^{-2} M) contained TMS dissolved in acetone-d_6 in the temperature range from 190 to 310 K, molar conductivity (YSI 3100 conductivity instrument with a 3253 cell Pt/Pt, K = 1.0 cm^{-1}) using acetonitrile as solvent at room temperature, and cyclic voltammetry (EG & G PAR potentiostat-galvanostat model 263A). All electrochemical measurements were performed in acetonitrile solution containing 0.1 M *N*-tetrabutylammonium tetrafluoroborate, $(C_4H_9)_4NBF_4$, as the supporting electrolyte. A typical three-electrode array was employed for all electrochemical measurements: platinum microdisk (Pt, 2.01 mm^2) as working electrode, Pt wire as counterelectrode, and a pseudoreference electrode of AgCl(s)−Ag(wire) immersed in an acetonitrile 0.1 M $(C_4H_9)_4NCl$ solution. All solutions were deoxygenated with N_2 before each measurement. All voltammograms were started from the current null potential ($E_{i=0}$) and were scanned in both directions, positive and negative. In agreement with IUPAC convention, the voltammogram of the ferrocene/ferricinium (Fc/Fc^+) system was obtained to establish the values of half wave potentials ($E_{1/2}$) from the expression $E_{1/2} = (E_{ap} + E_{cp})/2$. To obtain the normalized current for each complex, the measured current was divided by the exact molar concentration of the electroactive species.

Single-Crystal X-ray Diffraction. Diffraction data of prismatic crystals for the OCN^- (**4**) complex were collected at 298 K with an Enraf-Nonius CAD4 diffractometer using graphite-monochromated Mo Kα radiation (λ = 0.71073 Å), while for the I^- (**3**) and SCN^- (**5**) complexes, the data were collected at 298 K with a Bruker 6000 CCD area detector diffractometer and analyzed using monochromated Mo Kα radiation (λ = 0.71073 Å). Diffraction data for the Br^- (**2**), CH_3CN (**7**), and CN^- (**8**) complexes were collected at 298 K on a Siemens P4 diffractometer, using the standard procedure with monochromated Mo Kα radiation (λ = 0.71073 Å). A semiempirical ψ-scan absorption correction was applied to all the data. The structures were solved and refined without constraints or restraints. A minor disorder was observed in the hexafluorophosphate ions for all the reported compounds. All structures were solved by direct methods using SHELXS-97-2. Least-squares refinement based on F^2 was carried out by the full-matrix method with SHELXL-97-2.[13] All non-hydrogen atoms were refined with anisotropic thermal parameters. The hydrogen atoms for all the reported structures were located in the difference map and included in the refinement with an isotropic fixed thermal parameter using a "riding" model. Neutral atom scattering factors and anomalous dispersion corrections were obtained from the International Tables for Crystallography, Vol. A.[14] Unit cell parameters, along with data collection and refinement details, for all the reported complexes are listed in Table 1. Selected bond lengths of all the compounds are listed in Table 2. All molecular structure drawings were generated using the WINGX suite of crystallographic programs for Windows.[15] The labels of the coordinated atoms of bztpen used in all the studied compounds are shown in Scheme 1.

Results and Discussion

All synthetic procedures yielded compounds whose spectroscopic characterization, X-ray diffraction, and elemental analysis is indicative of complexes of Fe(II) with the general formula $[Fe(bztpen)X]^{n+}$. Because of the difficulty in precipitating the compounds with the BF_4^- counterion, exchange with PF_6^- was chosen to crystallize all compounds.

The IR spectra of all compounds confirm the coordination of the pentadentate ligand (bztpen) to the metal; in fact, all relevant ligand bands show shifts of ∼10−20 cm^{-1} in the 1600−1300 cm^{-1} range, when compared to those of the free ligand.[8] Additionally, all spectra clearly display the bands at 840 and 560 cm^{-1}, corresponding to the vibration modes for the octahedral hexafluorophosphate unit, PF_6^-, confirming its presence as counteranion of the cationic fragment. All compounds containing the nitrile group display the ν(CN) absorption in the 2200−2000 cm^{-1} range.[16] For the SCN^- (**5**) compound, a band is observed consisting of the overlapping of two absorptions occurring at 2052 and 2036 cm^{-1} and with almost identical intensity patterns. This is consistent with the existence of two cations in the unit cell with slightly different values for the Fe−NCS distances and angles. The OCN^- derivative (**4**) displays the largest ν(OCN) frequency value at 2212 cm^{-1}. When compared to the values observed for the SCN^- (**5**) compound, the larger value obtained for the OCN^- (**4**) compound must take into account the difference in mass of the oxygen atom relative to the sulfur atom because the ν(CN) vibration requires displacement of the CO and CS fragments in the triatomic ligand.

X-ray Structures of the Br^-(2), I^-(3), OCN^-,(4), SCN^-(5), CH_3CN (7), and CN^-(8) Hexafluorophosphate Derivatives. Structures were solved partly to study the effect on the coordination environment of the metal produced by each monodentate ligand. The magnetic, spectroscopic, and electrochemical properties can be greatly modified by these effects. The structures of the complexes with $X^- = Cl^-$, Br^- (as a perchlorate), and $N(CN)_2^-$ were reported in previous works.[6,10]

All complexes were solved at 298 K. Complexes **2**, **3**, and **4** are yellow and crystallize in the orthorhombic space group *Pbca*. Orange **5**, red brown **7**, and dark red **8** crystallize in the $P\bar{1}$ space group. All compounds have hexafluorophosphate counteranions which neutralize the charge of the complex cation. The compound with cyanide has water and

(11) Evans, D. F. *J. Chem. Soc.* **1959**, 2003−2005.
(12) Shubert, E. M. *J. Chem. Educ.* **1992**, *69*, 62−69.
(13) Sheldrick, G. M. *SHELX97, Programs for Crystal Structure Analysis*, release 97-2; Institüt für Anorganische Chemie der Universität: Göttingen, Germany, 1998.
(14) Hahn, T., Ed. *International Tables for Crystallography*; Kluwer Academic Publishers: Dordrecht, The Netherlands, 1995; Vol. A.
(15) Farrugia, L. J. *J. Appl. Crystallogr.* **1999**, *32*, 837−838.
(16) Nakamoto, K. *Infrared and Raman Spectra of Inorganic and Coordination Compounds*, 5th ed.; John Wiley & Sons: New York, 1997; Part B.

Table 1. Crystal and Structure Refinement Data for $[Fe(bztpen)X]^{+/2+}$ Cations

parameters	Br^- (**2**)	I^- (**3**)	OCN^- (**4**)	SCN^- (**5**)	CH_3CN^- (**7**)	CN^- (**8**)
space group	*Pbca*	*Pbca*	*Pbca*	$P\bar{1}$	*Pbca*	$P\bar{1}$
a (Å)	18.452	17.445	18.227	8.814	17.921	9.485
b (Å)	16.9375	18.465	17.703	18.842	18.913	10.877
c (Å)	18.471	18.465	18.250	19.003	19.744	16.570
α (deg)	90	90	90	91.12	90	73.26
β (deg)	90	90	90	95.70	90	81.56
γ (deg)	90	90	90	92.74	90	76.04
vol (cm^3)	5772.7	5947.98	5888.77	3135.78	6692.0	1610.43
Z	8	8	8	4	8	2
D_{calcd} (Mg m^{-3})	1.621	1.678	1.503	1.446	1.609	1.469
T (K)	298(2)	298(2)	298(2)	298(2)	298(2)	298(2)
μ(Mo Kα) (mm^{-1})	2.028	1.663	0.638	0.663	0.645	0.600
cryst size (mm)	0.5 × 0.5 × 0.5	0.4 × 0.2 × 0.15	0.4 × 0.2 × 0.2	0.1 × 0.1 × 0.1	0.4 × 0.2 × 0.2	0.6 × 0.4 × 0.1
θ range (deg)	1.97−25.99	1.95−24.00	1.95−26.69	2.15−24.07	2.15−27.48	1.29−29.00
total reflns	6712	24 393	40 513	16 912	14 246	9312
independent reflns	5562	4618	6205	9709	7603	7861
data/constraints/params	5562/0/370	4618/0/370	6205/0/385	9709/0/775	7603/0/452	7861/3/414
R1	0.0733	0.0473	0.0716	0.0545	0.0782	0.0582
wR2	0.1306	0.1275	0.2194	0.0807	0.2134	0.1465
$\Delta\rho_{max}$ (e $Å^{-3}$)	0.655	1.195	1.023	0.595	1.159	0.610
$\Delta\rho_{min}$ (e $Å^{-3}$)	−0.471	−0.498	−0.449	−0.267	−0.953	−0.483

Table 2. Selected Fe−L Bond Lengths (Å) and Distortion Parameter (Φ/deg) for $[Fe(bztpen)X]^{+/2+}$ Cations

	Cl^- (**1**)	Br^- (**2**)	I^- (**3**)	OCN^- (**4**)	SCN^- (**5**)	$N(CN)_2^-$ (**6**)	CH_3CN (**7**)	CN^- (**8**)
ref	6	this work	this work	this work	this work	10	this work	this work
Fe1−N1	2.228(3)	2.232(5)	2.209(5)	2.162(5)	2.187(5)	1.976(4)	1.975(4)	1.972(3)
Fe1−N2	2.254(3)	2.244(5)	2.226(4)	2.244(4)	2.252(4)	2.002(3)	2.000(4)	2.024(2)
Fe1−N3	2.175(3)	2.177(5)	2.172(4)	2.233(4)	2.174(5)	1.965(3)	1.971(4)	1.967(3)
Fe1−N4	2.288(3)	2.292(5)	2.283(4)	2.272(4)	2.245(4)	2.089(3)	2.077(4)	2.079(3)
Fe1−N5	2.279(3)	2.278(5)	2.269(5)	2.274(4)	2.241(4)	1.995(3)	1.994(4)	1.988(3)
[Fe−X]	2.329(1)	2.498(1)	2.720(1)	2.007(5)	2.026(5)	1.956(4)	1.925(4)	1.914(3)
$[Fe-N_5]_{average}$	2.245	2.245	2.232	2.237	2.220	2.005	2.003	2.006
$[Fe-L_6]_{average}$	2.259	2.287	2.313	2.199	2.188	1.997	1.990	1.991
Φ	7.84	8.29	8.70	7.21	8.51	3.04	2.66	2.75

Scheme 1. General Structure for bztpen Ligand and Numbering Scheme of the Coordinated Nitrogen Atoms

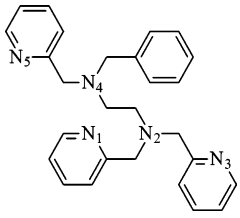

methanol crystallization molecules, and in this case, hydrogen bonds between water and methanol molecules were observed. In addition, the water molecules form four-membered rings with the nitrogen from the cyanide. The rest of the complexes show no solvent crystallization molecules.

Because there are no relevant intermolecular interactions, hydrogen bonding (except for **8**) or π stacking, in the cell, cohesion is attributed essentially to the electrostatic interaction of the $[Fe(bztpen)X]^+$ cations and the slightly disordered PF_6^- anions for the rest of the complexes.

Complexes **2**, **3**, **4**, **7**, and **8** consist of one [Fe(II)-(bztpen)X]$^{n+}$ cation per asymmetric unit, while complex **5** consists of two $[Fe(bztpen)SCN]^+$ equivalent cations in the asymmetric unit.

In all the complexes, the iron atom is in a slightly distorted octahedral $[FeN_5X]$ environment, where five of the nitrogen atoms belong to the pentadentate bztpen ligand, with an average Fe−N bond distance, $[FeN_5]_{average}$, shown in Table 2. The remaining coordination site in the $[FeN_5X]$ octahedron is occupied by iodide and bromide, for the monatomic anions, and the nitrogen atom for the OCN^- and SCN^- anions and the CH_3CN molecule. Coordination to the metal center occurs via the carbon atom for the CN^- anion. For all compounds obtained, monodentate coordination is observed. The total average bond distances in the octahedron, $[Fe-L_6]_{average}$, are shown in Table 2. In all complexes, the bztpen ligand envelops the iron atom defining a distorted square pyramid with the nitrogen atom N(2) lying on the axial apex. The N(2) atom is in the center of a tripod with a distance to the iron atom shown in Table 2; the arms of the tripod are defined by two picolylamine moieties [N(2)−C(6)−C(5)−N(1)] and [N(2)−C(7)−C(8)−N(3)] and one ethylenediamine moiety [N(2)−C(13)−C(14)−N(4)]. These arms are anchored to the iron atom by the N(1), N(3), and N(4) atoms. While N(1) is *trans* to the N(4) atom of ethylenediamine, the N(3) atom from the other picolylamine fragment is *trans* to the fifth nitrogen atom of the square pyramid, N(5). The X^- ligand is in a *trans* configuration to N(2). Fe−X bond distances are shown in Table 2. Bond angles around the iron atom show distortion from the expected 90 and 180° for a perfect octahedron. This distortion is imposed by the geometrical constraints of the pentadentate ligand, as well as by the characteristics of each X^- ligand.

The molecular structures of the CN^- (**8**) and the OCN^- (**4**) complexes are displayed in Figures 1 and 2, respectively, together with the atom numbering scheme for the octahedral site employed for all the described compounds. Relevant

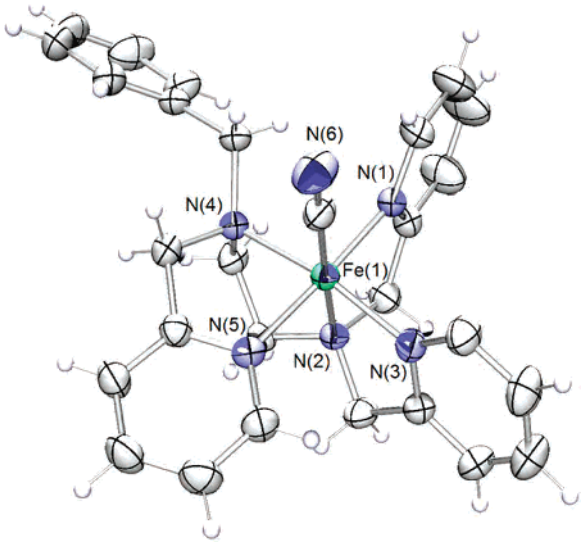

Figure 1. ORTEP diagram of the [Fe(bztpen)CN]PF_6 compound. The thermal ellipsoids are shown at 50% probability.

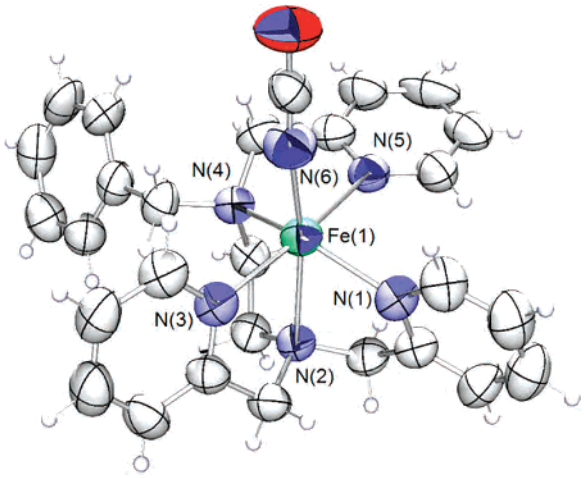

Figure 2. ORTEP diagram of the [Fe(bztpen)OCN]PF_6 compound. The thermal ellipsoids are shown at 50% probability.

crystal data for these complexes are shown in Table 1. CIF files of the six new complexes and ORTEP diagrams with the molecular structure for the rest of the reported compounds are included as Supporting Information.

The results in Table 2 show that, on the basis of the $[Fe-N_5]_{average}$ and $[Fe-L_6]_{average}$ bond distances, the compounds may be classified in two different groups. Although variations are observed in the magnetic, spectroscopic, and electrochemical properties for these two groups of compounds, it will be attempted to correlate structural parameters with each property to rationalize the observed effects arising from X^- substitution.

Magnetic Response and Structural Parameters. It is well-known that there is a clear relationship between the magnetic response of the octahedral complexes of Fe(II) and the metal ligand distances.[17,18]

The magnetic response of solid samples of the derivatives with Cl^-, Br^-, I^-, OCN^-, and SCN^- is paramagnetic in the whole temperature range, with an approximate magnetic moment value of 5.0 μ_B, corresponding to the high-spin (HS) configuration for Fe(II). The magnetic study of the latter complex from 300 to 1.8 K has been included in the Supporting Information. These compounds have a characteristic yellow color, except for the SCN^- which is orange. It must be mentioned, however, that the Br^- (**2**) complex with the perchlorate anion has been previously obtained[6] as paramagnetic brown crystals. The complexes with CN^-, CH_3-CN, and $N(CN)_2^-$ are diamagnetic with a magnetic moment value of ~0 μ_B, corresponding to the low-spin (LS) Fe(II) configuration. These crystals have a characteristic and very intense red-brown color. None of the compounds studied is a spin-crossover system.

As can be seen in Table 2, the $[Fe-N_5]_{average}$ distances for the paramagnetic complexes **1**, **2**, **3**, **4**, and **5** are in the range of 2.22−2.25 Å, while the diamagnetic complexes of **6**, **7**, and **8** are in the range of 2.00−2.01 Å. This trend is also observed for the $[Fe-L_6]_{average}$ distances, which are in the 2.19−2.31 Å range for the paramagnetic complexes and 1.99−2.01 Å for the diamagnetic complexes.

The analysis of bond angles around the Fe(II) ion shows a great deviation from the expected regular octahedron. The fact that the iron atoms in each complex are in a distorted octahedral environment, is imposed by two factors. First, the geometrical constraints imposed by the bztpen ligand and, second, the basicity of the monodentate anion. The trigonal distortion parameter Φ as defined by Purcell[19] and used by McCusker[20] has been calculated to arrive at a quantitative measurement regarding the extent of distortion for each compound. [The average trigonal distortion parameter can be defined as $\Phi = \sum_{\theta=1}^{24}(|60 - \theta|)/24$, where θ represents the trigonal complementary angles of all triangles defined by eight faces of the octahedron, yielding a total of 24 trigonal angles.] Calculated values for this parameter are shown in Table 2.

Once again, two distinct groups appear: the first in the 7.21−8.70° range and the second in the 2.66−3.04° range. The former group corresponds to HS Fe(II) complexes, while the latter group corresponds to the LS Fe(II) complexes.[18,20,21]

The average bond distances, $[Fe-N_5]_{average}$ and $[Fe-L_6]_{average}$, and the trigonal distortion parameter Φ, thus appear to be directly related to the magnetic properties of the complexes.[17,18,21]

From the above discussion, it seems clear that structural parameters are useful in pointing out the existence of two groups of complexes. To determine if there is any modulation of the electronic properties caused by the monodentate ligands, both the spectroscopic study and the electrochemical behavior of all complexes is required.

Solution Studies. All complexes were characterized using UV−vis spectroscopy and cyclic voltammetry. In addition, a solution study of the magnetic properties in acetonitrile

(17) Gütlich, P.; Hauser, A.; Spiering, H. *Angew. Chem., Int. Ed. Engl.* **1994**, *33*, 2024−2054.
(18) Hauser, A. *Top. Curr. Chem.* **2004**, *233*, 49−58.
(19) Purcell, K. F. *Am. Chem. Soc.* **1979**, *101/18*, 5147−5152.
(20) McCusker, J. K.; Rheingold, A. L.; Hendrickson, D. N. *Inorg. Chem.* **1996**, *35*, 2100−2112.
(21) Guionneau, P.; Marchivie, M.; Bravic, G.; Létard, J.-F.; Chasseau, D. *Top. Curr. Chem.* **2004**, *234*, 97−128.

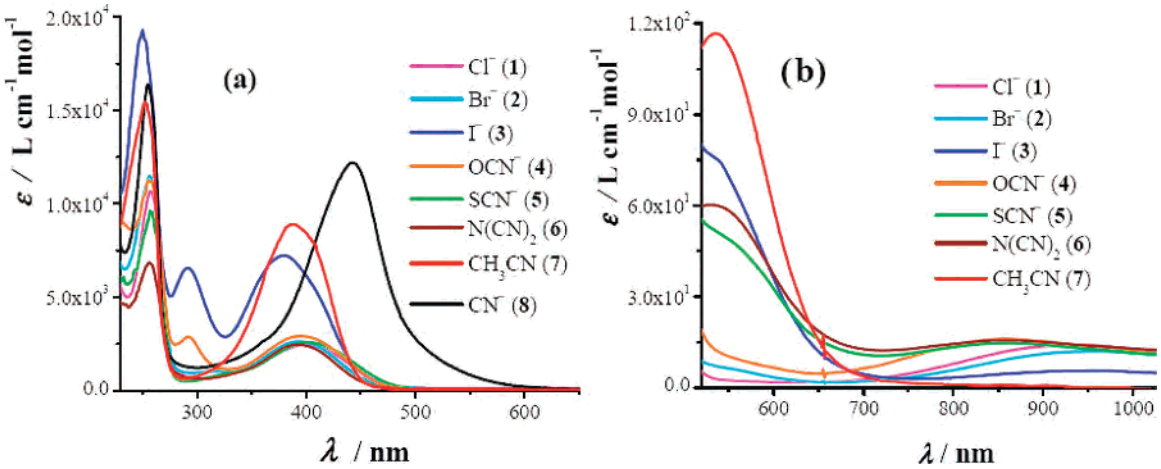

Figure 3. UV−vis spectra of [Fe(bztpen)X]PF_6 compounds in CH_3CN solutions obtained in the ranges of (a) 190−600 nm and (b) 500−1100 nm.

Table 3. Molar Absorption Coefficients for [Fe(bztpen)X]$(PF_6)_n$ Compounds in CH_3CN Solutions at 293 K[a]

	charger tranfer (CT)			d−d		
	λ_{max} (nm)	ν (cm^{-1})	ϵ (L cm^{-1} mol^{-1})	λ_{max} (nm)	ν (cm^{-1})	ϵ (L cm^{-1} mol^{-1})
CH_3CN (**7**)	252	39 682	15 425			
	390	25 641	8892			
	535	18 692	117			
I^- (**3**)	380	26 316	7233	959	10 428	5.6
	542	18 450	77			
Br^- (**2**)	392	25 510	2626	959	10 428	12.0
Cl^-(**1**)	400	25 000	24 572	929	10 764	14.0
OCN^- (**4**)	404	24 752	2569	860	11 628	16.0
SCN^- (**5**)	394	25 381	2903	858	11 655	14.7
	531	18 832	53			
$N(CN)_2^-$ (**6**)	393	25 445	2461	860	11 628	15.6
	529	18 903	60			
CN^- (**8**)	443	22 573	12 295			

[a] The absorptions correspond to charge-transfer band (CT) and d−d bands.

Table 4. Voltammetric Parameters and Percentage of Dissociation (% dissoc) Data for ~10^{-3} M [Fe(bztpen)X]$^+$ in Acetonitrile Solutions[a]

	E_{pa} (V)	E_{pc} (V)	i_{pc}/i_{pa}	E_p (V)	$E_{1/2}$ (V)	$E_{1/2}{}^b$ (V)
CH_3CN (**7**)	0.613	0.539	0.90	0.074	0.576	0.000
I^- (**3**)	0.387	0.313	−	0.074	0.350	0.226
Br^- (**2**)	0.297	0.213	0.88	0.084	0.255	0.321
Cl^- (**1**)	0.253	0.179	0.75	0.074	0.216	0.360
OCN^- (**4**)	0.181	0.109	0.70	0.072	0.145	0.431
SCN^- (**5**)	0.267	0.179	0.98	0.088	0.223	0.353
$N(CN)_2^-$ (**6**)	0.400	0.312	0.93	0.088	0.356	0.220
CN^- (**8**)	−0.040	−0.108	0.93	0.070	−0.074	0.650

[a] All potential values are in V vs Fc^+−Fc. [b] $\Delta E_{1/2} = E_{1/2} - E^\circ_{1/2}$, where $E_{1/2}$ is the half wave potential for X^- derivatives and $E^\circ_{1/2}$ is that for the CH_3CN derivative).

for the diamagnetic compounds **7**, **8**, and **6** was carried out employing the variable-temperature NMR Evans method. While the diamagnetic character of the first two complexes was confirmed, the latter compound becomes paramagnetic in solution but displays a slight, smooth spin transition as the temperature decreases (310−190 K); this probably caused by the relaxation of the octahedral environment produced by the solvation of the complex cation.

Electronic Absorption Spectra. A very important feature of the Fe(II) complexes is that, because of their electronic structure, the paramagnetic complexes always present a d−d band in the visible region, while this band is absent in the diamagnetic complexes. The spectra obtained in acetonitrile solutions of each Fe(II) compound are shown in Figure 3a in the ultraviolet region and 3b in the visible region.

The observed maxima with its respective molar absorption coefficients, ϵ (L mol^{-1} cm^{-1}), are shown in Table 3. Each spectrum displays an absorption maximum at wavelength, λ, ≈ 390 nm (25 641 cm^{-1}), with a molar absorption coefficient (ϵ (L cm^{-1} mol^{-1})) of ~10^4. These absorptions are usually associated to MLCT (metal ligand charge transfer) transitions for Fe−bztpen, $t_{2g}-\pi_L{}^*$.[22]

For all the paramagnetic compounds in solution, the absorption maxima associated with the d−d transition in solution was observed at a λ value in the range from 860 nm (11 628 cm^{-1}) to 959 nm (10 428 cm^{-1}), with molar absorption coefficients values (ϵ) that fall in the range from 16.0 to 5.6 L cm^{-1} mol^{-1}. This behavior is typical of high-spin octahedral Fe(II) compounds. Molar absorption coefficients and their associated d−d frequency values for each compound are shown in Table 3. The observed shifts to larger frequency values, corresponding to the d−d absorption in all the studied complexes, confirm the relative stability order also observed in the structural analysis and magnetic behavior.

The spectroscopic UV−vis experiments show that complexes **1**−**5** present the expected d−d transition for HS Fe(II) compounds, whereas complexes **7** and **8** do not exhibit such a transition. However, complex **6** does exhibit a d−d transition, suggesting that the spin state of this complex in solution is altered because of solvent effects.

The NMR Evans method was employed to evaluate the nature of this change, and the aforementioned transition was found in the studied temperature range. While the displacement obtained for the TMS signal confirmed the diamagnetic behavior of complexes **7** and **8**, for compound **6**, the magnetic moment value estimated from the observed displacement of the TMS signal is 5.0 μ_B at room temperature, corresponding to the high spin (HS) state for Fe(II), and ~0.6 μ_B at 190 K.

(22) Lever, A. B. P. *Inorganic Electronic Spectroscopy*, 2nd ed.; Elssevier: New York, 1986; pp 457−470.

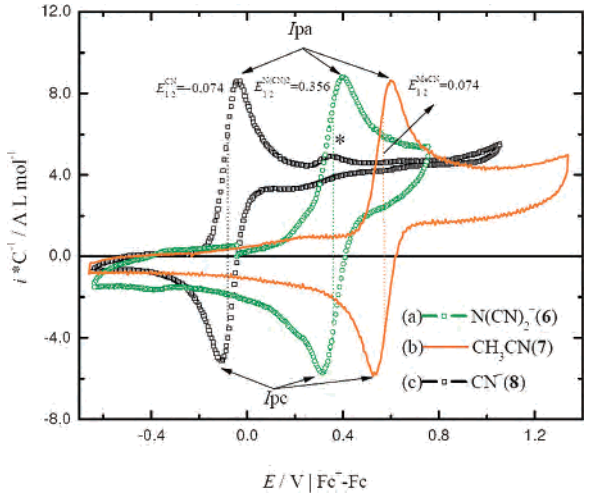

Figure 4. Typical cyclic voltammograms obtained for ~1.0 mM (a) [Fe(bztpen)N(CN)$_2$]PF$_6$, (c) [Fe(bztpen)CN]PF$_6$, and **(b)** [Fe(bztpen)CH$_3$CN](PF$_6$)$_2$ in 0.1 M of Bu$_4$NPF$_6$ acetonitrile solution at 100 mV s^{-1} on a carbon glass electrode. In all cases, the potential scan was initiated in the positive direction from $E_{i=0}$.

Electrochemistry (Cyclic Voltammetry). The analysis of the complexes with only one typical monoelectronic quasi-reversible process will be discussed initially, followed by the analysis of those systems which exhibit additional redox processes. The study of the complex with N(CN)$_2^-$ (**6**) is reported elsewere.[10]

The complexes with N(CN)$_2^-$ (**6**), CH$_3$CN (**7**), and CN$^-$ (**8**), see Figure 4, exhibit a voltammogram with only one quasi-reversible process (I), according to the i_{pc}/i_{pa} ratio shown in Table 4. From the values obtained for difference between anodic and cathodic peak potentials (ΔE_p), it is possible to suggest that only one electron-transfer processes take place (ΔE_p = 0.074, 0.088, and 0.070 V respectively, see also Table 4). Half-wave potential values ($E_{1/2}$) for these complexes are also shown in Table 4.

For the CN$^-$ (**8**) complex (Figure 4c), the voltammogram displays an oxidation signal with an anodic peak potential of $E_{pa} = -0.040$ V. A reduction signal appears at a cathodic peak potential of $E_{pc} = -0.108$ V. The difference between both values is $\Delta E_p = 0.070$ V, and the half wave potential value is $E_{1/2} = -0.074$ V. The ratio of cathodic (i_{pc}) and anodic (i_{pa}) peak current values is $i_{pc}/i_{pa} = 0.93$. Analysis of the redox process for compound **8** confirms that it is a quasi-reversible one-electron transfer process. The asterisked (*) signal that appears at $E_{ap} = 0.253$ V, belongs to the Cl$^-$ derivative, employed in the synthesis of **8**.

The voltammograms of the complexes of Cl$^-$ (**1**), Br$^-$ (**2**), OCN$^-$ (**4**), and SCN$^-$ (**5**), Figure 5a, and the ΔE_p and i_{pc}/i_{pa} ratios obtained are consistent with monoelectronic quasi-reversible processes equivalent to the one previously described. The corresponding $E_{1/2}$ values are shown in Table 4. However, these voltamperograms also show another process (II) which is, in all cases, less intense. This process is also quasi-reversible and has $E_{1/2} = 0.570$ V (Figure 5a).

Finally, the voltammogram for the I$^-$ (**3**) complex (Figure 5b) displays three oxidation and four reduction signals. The main process appears at $E_{1/2} = 0.570$ V and is labeled as II.

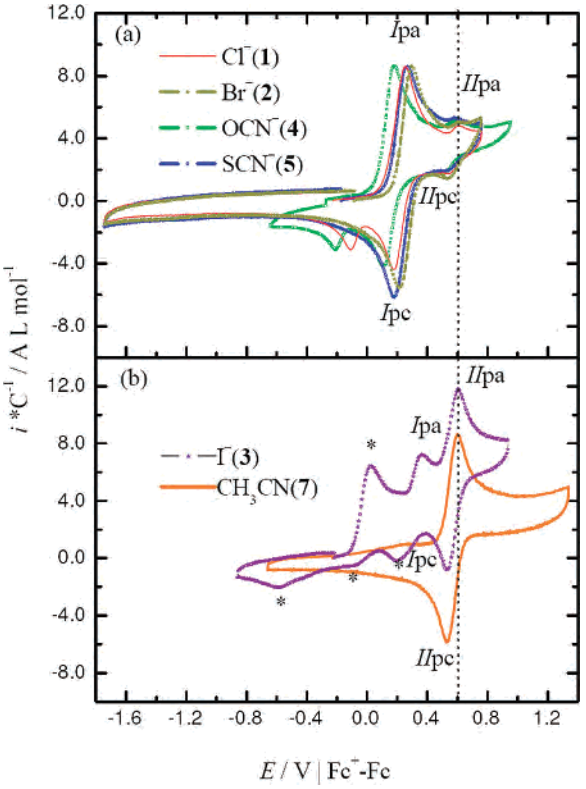

Figure 5. Typical cyclic voltammograms obtained for ~1.0 mM of the (a) Cl$^-$, Br$^-$, OCN$^-$, and SCN$^-$ derivatives and the (b) I$^-$ and CH$_3$CN derivatives in 0.1 M Bu$_4$NPF$_6$ acetonitrile solution at 100 mV s^{-1} on a carbon glass electrode. In all cases, the potential scan was initiated in the positive direction from $E_{i=0}$.

However, there is another process in $E_{1/2} = 0.350$ V identified as I. Along with these two processes, there are also one oxidation and at least three reduction signals. Values of $E_{1/2}$, i_{pc}/i_{pa}, and ΔE_p were obtained for each complex and are shown in Table 4.

Because of the similarity of the $E_{1/2}$ values for the processes labeled as II with the process observed for the acetonitrile complex, it is possible to suggest the presence of the [Fe(bztpen)CH$_3$CN] complex in the solutions of **1**−**5**.

It follows that this signal is produced as a result of the dissociation of each complex in the acetonitrile solution, according to the equation

$$[Fe^{II}(bztpen)X]^+ + CH_3CN = [Fe^{II}(bztpen)CH_3CN]^{2+} + X^-$$

Consequently, process I can be assigned to the [Fe(III)(bztpen)X]$^{2+}$/[Fe(II)(bztpen)X]$^+$ system in all complexes. The remaining observed signals for complex **3** can be attributed to the free iodide anion, which is electroactive in these conditions. The electrochemical study of a 1 mM KI solution (not shown) was performed, and those signals labeled with an asterisk (*) belong to the free iodide (I$^-$) oxidation and reduction processes (Figure 5b.)

To explain these results quantitatively, the normalized anodic intensity for both signals (I, i_{Ipa}, and II, i_{IIpa}) obtained for each complex is required. From these data, the percentage of dissociation for each complex was obtained employing the equation

$$\% \text{ dissoc} = \frac{i_{\text{IIpa}}}{i_{\text{Ipa}} + i_{\text{IIpa}}} \times 100$$

The calculated value for each complex is shown in Table 5. The values obtained fall in the range of 8−12% for the Cl^- (**1**), Br^- (**2**), OCN^- (**4**), and SCN^- (**5**) compounds. However, the value for the I^- (**3**) complex is as large as 69%, indicating that $[Fe(bztpen)I]^+$ is highly dissociated and that roughly 31% of the undissociated species remains in solution.

This fact was confirmed by obtaining the molar conductivity value (Λ) of an approximately 1 mM acetonitrile solution of the CH_3CN (**7**) and I^- (**3**) complexes, where the value of 264 S $mol^{-1}cm^2$ obtained for compound **7** is consistent with a 2:1 electrolyte. However, the value of 186 S $mol^{-1}cm^2$ obtained for compound **3** is greater than the expected value for a 1:1 electrolyte and corresponds to approximately 2/3 of the iodide dissociated from the complex.

The percentage of dissociation (% dissoc) represents a quantitative measurement of the relative stability of a $[Fe(bztpen)X]^+$ complex in solution. From these values, the corresponding formation equilibrium constant for each complex can be obtained (see Table 5) according to the equilibrium

$$Fe(II)LS + X^- = Fe(II)LX + S$$

$$K^{Fe^{II}LX}_{Fe^{II}L,X} = \frac{[Fe(II)LX]^+}{[Fe(II)LS]^{2+}[X^-]}$$

The $N(CN)_2^-$ (**6**) and CN^- (**8**) derivatives show no trace of the signal associated with the $[Fe(bztpen)CH_3CN]^{2+}$ species. In this case, the sensitivity of the voltammetric experiment does not allow for the estimation of this quantity. Consequently, it is feasible to assume that the equilibrium constant for these two compounds is much larger than 10^5.

Shifts in the $E_{1/2}$ value for the $[Fe(bztpen)X]^+$ compounds can be obtained in terms of the Nernst equation, from the $E^\circ_{1/2}$ value for the $[Fe(bztpen)CH_3CN]^{3+}/[Fe(bztpen)CH_3CN]^{2+}$ redox pair, and the stability constants of the $[Fe(bztpen)X]^{2+}$ and $[Fe(bztpen)X]^+$ systems. The resulting expression is

$$E_{1/2} = E^\circ_{1/2} - \frac{\mathscr{R}T}{n\mathscr{F}} \ln \frac{K^{Fe^{III}LX}_{Fe^{III}L,X}}{K^{Fe^{II}LX}_{Fe^{II}L,X}}$$

From this equation, the ratio of the equilibrium constants may be obtained by the calculated values of $\Delta_{E_{1/2}} = E_{1/2} - E^\circ_{1/2}$. The ratio values at 293 K for each derivative are shown in Table 5. From this ratio and the values obtained for the Fe(II) formation constant $K^{Fe^{II}LX}_{Fe^{II}L,X}$, the corresponding value of the Fe(III) formation constant $K^{Fe^{III}LX}_{Fe^{III}L,X}$ can be determined (Table 5). For the paramagnetic derivatives, the Fe(II) equilibrium constant was higher than the corresponding Fe(III) constant. For the $N(CN)_2^-$ (**6**) derivative, the lowest $\Delta E_{1/2}$ value was obtained, indicating that the stability of the Fe(II) and Fe(III) complexes is similar. Considering that $K^{Fe^{II}LX}_{Fe^{II}L,X} > 10^5$ and that $\Delta E_{1/2} = 0.220$ V, we can conclude that the Fe(III) complex has a $K^{Fe^{III}LX}_{Fe^{III}L,X} > 10^6$ for this derivative.

Table 5. Values of Dissociation Percent and Estimated Formation Equilibrium Constants for All Complexes in Acetonitrile Solution at 293 K

	% dissoc	$K^{Fe^{II}LX}_{Fe^{II}L,X}$	$(K_f^{Fe^{III}LX})/(K_f^{Fe^{II}LX})$	$K^{Fe^{III}LX}_{Fe^{III}L,X}$
CH_3CN (**7**)				
I^- (**3**)	68.7	$10^{2.8}$	$10^{3.9}$	$10^{1.0}$
Br^- (**2**)	11.1	$10^{4.9}$	$10^{5.5}$	$10^{0.6}$
Cl^- (**1**)	10.8	$10^{4.9}$	$10^{6.1}$	$10^{1.3}$
OCN^- (**4**)	7.90	$10^{5.2}$	$10^{7.4}$	$10^{2.2}$
SCN^- (**5**)	8.60	$10^{5.1}$	$10^{6.0}$	$10^{0.9}$
$N(CN)_2^-$ (**6**)	≪8	≫10^5	$10^{3.8}$	≫10^9
CN^- (**8**)	≪8	≫10^5	$10^{11.1}$	≫10^{16}

With the above arguments, the equilibrium constant for the CN^- derivative of Fe(III) is the highest ($K^{Fe^{III}LX}_{Fe^{III}L,X} > 10^{16}$).

If the stability constant of Fe(III) with X^- is larger than that for Fe(II), the $E_{1/2}$ value will be lower than the $E^\circ_{1/2}$ value. Hence, the more stable the generated Fe(III) complex, the larger the difference will be between $E_{1/2}$ and $E^\circ_{1/2}$. The differences obtained for these compounds follow the trend described in the literature for similar systems.[23]

Conclusions

The synthesis and complete characterization of five new complexes of Fe(II) with general formula $[Fe(bztpen)X]PF_6$, where bztpen is the pentadentate ligand *N*-benzyl-*N*′,*N*′-tris (2-methylpyridyl)-ethylenediamine and X^- is an anionic monodentate ligand, Br^-, I^-, OCN^-, SCN^-, and CN^- (**2**, **3**, **4**, **5**, and **8**, respectively), and $[Fe(bztpen)CH_3CN](PF_6)_2$ (complex **7**) were achieved. All compounds were analyzed, including previously reported Cl^- (**1**) and $N(CN)_2^-$ (**6**) derivatives.[6,10] Spectroscopic and X-ray structural analyses show that all compounds are composed of the monomeric $[Fe(bztpen)X]^{n+}$ unit neutralized with PF_6^- anions.

From the analysis of the crystallographic parameters, it is clear that distortion of the octahedral coordination environment for the metal center is greater for compounds **1**−**5** than for compounds **6**−**8**, as shown by the larger values of Φ and the longer $[Fe-L_6]_{average}$ distances obtained for the former group of compounds than for the latter.

The observed magnetic susceptibility behavior in solid-state experiments shows that complexes **1**−**5** are all paramagnetic, while **6**−**8** are diamagnetic.

The spectroscopic UV−vis experiments show that complexes **1**−**5** present the expected d−d transition for HS Fe(II) compounds, while complexes **7** and **8** do not exhibit such a transition. However, complex **6** does present a d−d absorption, suggesting a change in its spin state caused by the solvent effect. This was confirmed with the NMR Evans technique in acetone solution of this complex and was also used to corroborate the diamagnetic behavior of complexes **7** and **8**.

(23) Howker, P. N.; Twigg, M. V. *Comprehensive Inorganic Chemistry*; Wilkinson, G., ed.; Pergamon: Oxford, 1987; Vol. IV, pp 1179−1288.

From these results, it is possible to conclude that the observed properties are imposed not only by the geometrical constraints of the pentadentate ligand and the characteristics of the monodentate ligand X^- but also by the solvent effect.[24]

Values of $E_{1/2}$ for the the Fe(III)/Fe(II) redox systems verify that the least-stable Fe(II) compound is **3**, while the most-stable compound is **8**.

From the normalized anodic intensity of the acetonitrile complex signal observed in the voltammogram for each complex, it is possible to obtain the percentage of dissociation for complexes **1**−**5**. From this estimate, the stability constant for the Fe(II) complexes is consistent with the trend established by the spectrochemical series. To improve the discussion concerning the relative stability of these systems, a comparison of the half-wave potentials differences ($\Delta E_{1/2}$) of all the complexes was performed. The analysis of these values establishes that the largest difference is obtained for the most stable Fe(III) complex, as expected for the derivative with CN^- ligand ($\Delta E_{1/2} = 0.650$ V). The lowest difference corresponds to the I^- derivative, which is the least stable of all the compounds: a fact that is consistent with the previously mentioned results. Additionally, the $N(CN)_2^-$ derivative is the most stable of the Fe(II) compounds in regard to its stability toward oxidation by O_2.

Acknowledgment. We thank the Universitat de Valencia-UNAM agreement for a predoctoral fellowship (N.O.V.). We are grateful to M. en C. Rosa Isela del Villar for NMR spectra studies, to Q. Marisela Gutierrez Franco for the IR spectra, and to Dr. Gerardo Medina-Dickinson for his kind revision of this manuscript.

Supporting Information Available: Figures S1−S5 and validated CIF files. This material is available free of charge via the Internet at http://pubs.acs.org.

IC0620743

(24) Murray, K. S.; Kepert, C. J. *Top. Curr. Chem.* **2004**, *233*, 195−228.